

# Model Validation of a Three-Phase Inverter EMT Model in DIgSILENT Power Factory

Anima Ganeshan  
School of Engineering  
RMIT University  
Melbourne, Australia  
anima.ganeshan@rmit.edu.au

Lasantha Meegahapola  
School of Engineering  
RMIT University  
Melbourne, Australia  
lasantha.meegahapola@rmit.edu.au

B.P McGrath  
School of Engineering  
RMIT University  
Melbourne, Australia  
[brendan.mcgrath@rmit.edu.au](mailto:brendan.mcgrath@rmit.edu.au)

D.G Holmes  
School of Engineering  
RMIT University  
Melbourne, Australia  
grahame.holmes@rmit.edu.au

**Abstract**— Ongoing global efforts to reduce carbon emissions are leading to a technological transformation of electrical grids from fossil fuel energy production using rotating machines, to renewable energy production using power electronic converters. However, conventional power system modelling and simulation approaches (i.e. root-mean-square strategies) are unable to adequately analyse power system dynamics with grid connected inverters. This is because accurate representation of the transient behaviour of a physical inverter system requires a high-resolution detailed time domain inverter simulation model. This paper presents a discrete-time approach to modelling such a grid connected inverter system, which accurately represents its transient response using an electromagnetic transient (EMT) DIgSILENT Power Factory model of a three-phase grid-connected inverter, current regulated in the synchronous reference frame (SRF). The performance of the developed EMT model has been confirmed by comparison against a known, and previously experimentally validated, time domain inverter model developed in PSIM.

**Keywords**— Discrete integrator, electromagnetic transient (EMT) modelling, three-phase inverter, LCL filter.

## I. INTRODUCTION

The electrical energy sector is currently undergoing a major technological transformation to meet renewable energy targets, with large numbers of renewable energy sources such as PV and wind now routinely connected to a grid using power electronic inverters. However, while grid connection of renewable generation is in general reasonably well governed by the National Electricity Rules and Grid Codes [1], the integration of power electronic converter (PEC) interfaced renewables to a synchronous generator dominant utility grid often experiences significant technical difficulties [2]. Hence accurate modelling of power electronic converters (PEC) for power system studies is of immense interest for the power utility sector to address this issue.

The proliferation of grid-connected PEC-based distributed generators (DG) in an utility grid necessitates the effective representation of inverters in power system dynamic studies. Many power system analysis packages model inverters as simplified voltage/current sources without detailed control schemes, for steady-state power system studies. They are either represented as a voltage source with a reactance in series or current source in parallel to a reactance, in such studies [3]. Dynamic studies of large power systems involve the detailed modelling of generator characteristics and controllers, along with their energy sources (such as exact turbine models for

synchronous generators). In contrast, the dynamics of a grid-connected DG are determined almost entirely by its internal control structure, which is typically implemented using cascaded controllers with a high-speed current regulator in the innermost control loop.

Dynamic studies of synchronous generator dominated large power networks are typically done using simulation packages, such as PSSE, DIgSILENT Power Factory, PSCAD, and ETAP, which solve a system of nonlinear equations in the 50Hz RMS phasor domain [4]. However, since the transient performance of inverters is determined by controllers operating in a micro-second timeframe, the transient performance of inverters using root-mean-square (RMS) models are unsatisfactory [5]. Hence it is necessary to model the inverters in the time domain using the electromagnetic transient (EMT) tools of PSCAD and DIgSILENT Power Factory, for power system dynamic studies. Unfortunately the difficulty in obtaining exemplary power electronic converter models from the manufacturers has led to the recent industrial practice of including inverter dynamic link library (DLL) wrapped code into power system transient study models [6]. Some of the EMT inverter models reported in the literature also follow a bottom-up approach [7], as opposed to the existing industrial practice, starting with the modelling of the most basic subsystem, and then identifying the large system as the interconnection of the basic subsystems. Finally, most EMT models reported to-date are based on reference power electronic controllers modelled in the continuous time domain [8].

This paper now presents an improved method for the bottom-up modelling of grid-connected DG inverter controllers, where the DIgSILENT Power Factory EMT model is built with the discrete-time functions of DIgSILENT Power Factory to match a discrete-time PSIM reference simulation model. The exemplary performance of the discrete-time domain inverter controller PSIM simulation model, which accurately models the transient response of an experimental inverter and controller, has been previously discussed in [9]. In this paper, the performance of the developed EMT model is benchmarked against this PSIM simulation model. The modelling approach presented in this paper serves as a contemplative approach to the accurate modelling of inverters for power system dynamic studies.

## II. THREE INVERTER MODEL SPECIFICATION

### A. Three-phase inverter model specification

The general circuit diagram of a grid-connected three-phase inverter is shown in Fig. 1, where the switching model of the three-phase grid-connected inverter power stage is built in PSIM as shown. The inverter-side inductor three-phase current quantities  $i_a, i_b, i_c$  are sampled at twice the switching frequency, converted into the synchronous frame and provided as input feedback signals to the current controller. The general design principles for this inverter are summarised below, with the parameters for the system modelled in this paper listed in Table I.

### B. LCL Filter Design

Three-phase grid connected inverters are typically interfaced to a utility grid by LCL filters, which can be designed using

$$L = \frac{V_{dc}}{24f_s \Delta i_{1max}} \quad (1)$$

where  $L$  is the inverter side inductance,  $V_{dc}$  is the DC link voltage,  $f_s$  is the switching frequency of the inverter,  $\Delta i_{1max}$  is the maximum permissible inductor current ripple.

and

$$C = x\% \frac{S}{2\pi f_o V_{ll}^2} \quad (2)$$

where  $C$  is the filter capacitance,  $S$  is the apparent power of the inverter,  $f_o$  is the fundamental grid frequency,  $V_{ll}$  is the rated line to line inverter rms voltage and  $x\%$  is the allowable percentage of the base capacitance [10].

Assuming  $\Delta i_{1max} = 7\%$  and  $x\% = 5\%$  and substituting these values and the system parameters from Table I into (1) and (2) the values of inverter side inductance and filter capacitance are obtained as  $L = 3\text{mH}$  and  $C = 10\mu\text{F}$ . The total inductance of the filter is chosen to be less than 10% of the base impedance. Hence the grid side inductance  $L_g = 1.65\text{mH}$  can be calculated as 3% of the base impedance. The attenuation admittance of the LCL filter is then given by

$$Y(s) = \frac{1}{s^3 L L_g C + s(L + L_g)} \quad (3)$$

which has the Bode plot characteristic shown in Fig. 2.

### C. Design of Synchronous Frame Current Regulator

The inverter side inductor current is regulated by a synchronous frame PI current regulator as shown in Fig. 3. The current controller is defined by

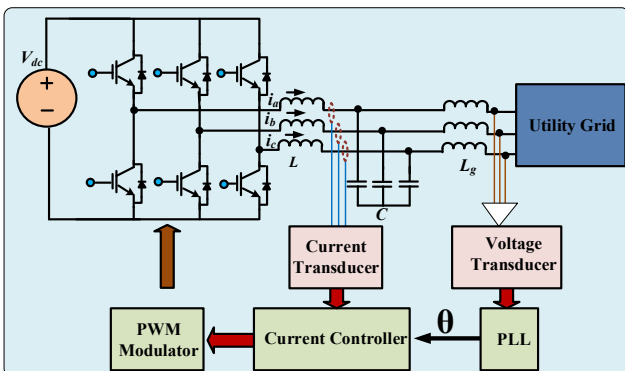


Fig. 1: Grid connected three phase inverter.

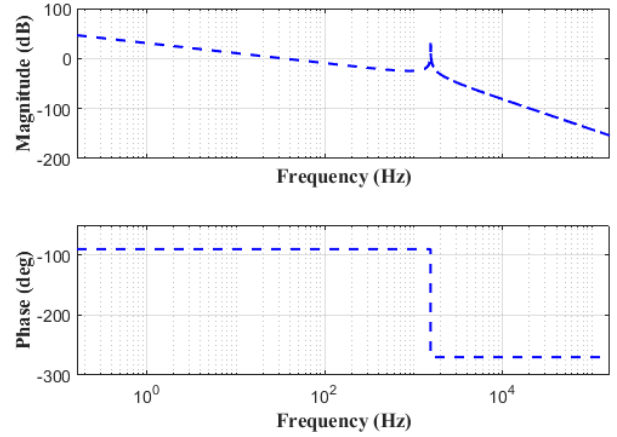


Fig. 2: Bode Plot of LCL filter attenuation admittance.

$$G_{c,inv} = K_p \left( 1 + \frac{1}{sT_i} \right) \quad (4)$$

The design of controller gains is discussed in [11]. The discrete-time implementation of the inverter synchronous frame current controller of Fig. 3 is shown in Fig. 4. The PLL and PI current regulators are built by discrete-time functional blocks such as sample and hold, integrator, delay. The model also implements the discrete anti-windup strategy described in [12], as shown in Fig. 4.

## III. DIGSILENT POWER FACTORY INVERTER MODEL

### A. Single-line diagram of the inverter model

The single line diagram is constructed in DiGSILENT Power Factory using the network elements available in the DiGSILENT Power Factory library. The single line diagram of three-phase grid connected inverter power stage of Fig. 1 is shown in Fig. 5. The inverter is modelled with the 'PWM converter with two DC connections' network element. The DC connections of the inverter network element are made to the 'DC source network' element. The LCL filter is built with the Common Impedance (i.e.,  $L$  and  $L_g$ ) and Shunt/Filter ( $C$ ) network elements as shown in Fig. 5. The LCL filter values used in the DiGSILENT Power Factory model are given in Table II. The inverter controller is modelled using the dynamic modelling approach in DiGSILENT Power Factory as discussed in the next section.

#### 1) DSL Model Frame and Components

The controller model equations are modelled using the DiGSILENT Power Factory simulation language (DSL). The basic development of dynamic model for the PSIM controller of Fig. 1 is shown in Fig. 6. The blocks are arranged to aid the logical flow of the basic development process. The initial step for dynamic modelling is to build a composite frame; a

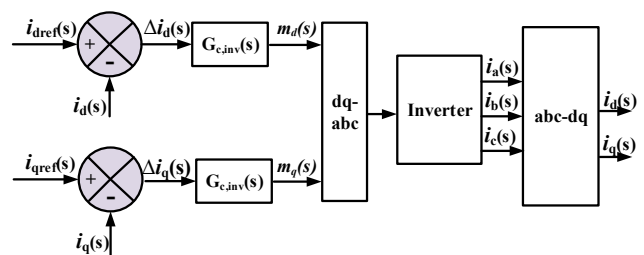


Fig. 3: Block diagram of inverter SRF PI controller.

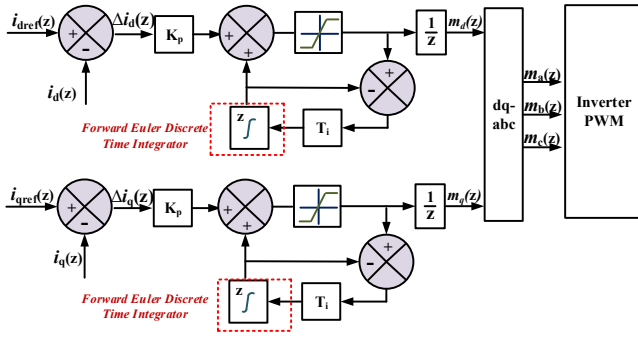


Fig. 4: Implementation of inverter SRF PI controller implementation in discrete time domain.

platform which gives an overview of the input/output signal interconnections of the frame slots. The composite frame of the inverter controller is shown in Fig. 6. The composite frame consists of inbuilt slots, such as the inverter plant slot, the PLL slot, the current measurement slot, the sample and hold slot and the clock. The frame also shows user defined slots for the PI controller and the reference generator. The reference current generation common model and the PI controller common model then follows, as described in the next section. The sampling frequency ( $f_{samp}$ ) of the controller is defined at the clock element (by setting clock frequency to 20 kHz). The PLL object, the sample and hold, and the current measurement object are configured similarly according to the model requirements.

### B. Reference Current Generation Model

The reference current generation model converts the sampled inverter currents  $i_a, i_b, i_c$  to the synchronous reference frame quantities ( $i_d, i_q$ ).  $i_d, i_q$  are then multiplied by a scaling factor ( $K\_scale$ ), as shown in Fig. 7, which is numerically equal to the peak value of the base current. The base current calculation for the DIgSILENT Power Factory power system model is given by

$$I_{base} = \frac{S}{\sqrt{3}V_{ll}} \quad (5)$$

Table I Inverter Parameters

Parameters	Symbol	Value
Rating of the VSC	S	10kVA
Rated line to line voltage of the VSC	$V_{ll}$	415V
Fundamental frequency of the grid	$f_0$	50Hz
DC link voltage of the VSC	$V_{dc}$	700V
Switching frequency	$f_s$	10kHz
Sampling Frequency	$f_{samp}$	20kHz

Table II DIgSILENT PF System Parameters

System Parameters			Formula	DIgSILENT PF entry
Inverter side filter inductance	$L$	3mH	$\frac{L2\pi f_0}{Z_{base}}$	0.0547 p.u.
Inverter filter capacitance	$C$	10 $\mu$ F	$C2\pi f_0$	3141.59 $\mu$ S
Grid side filter inductance	$L_g$	1.65mH	$\frac{L_g2\pi f_0}{Z_{base}}$	0.0301 p.u.
Inductor internal resistance	$r_l$	50m $\Omega$	$\frac{r_l}{Z_{base}}$	0.0029036 p.u.

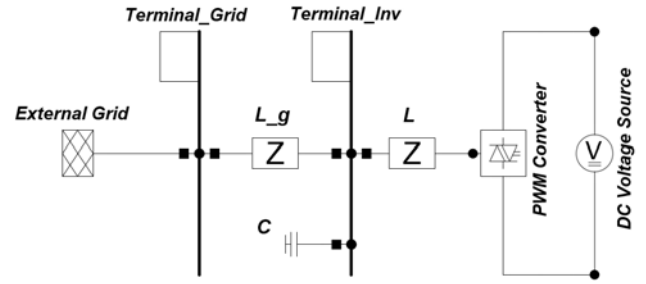


Fig. 5: Single Line Diagram (SLD) of grid connected three phase inverter.

Substituting the values into (5) from Table I,  $I_{base}$  for the DIgSILENT Power Factory model is 13.91A. This gives a base peak-current of 19.68A, which is rounded off to 20A. Hence the scaling factor ( $K\_scale$ ) of Fig. 8 is set to 20. The model is initialised at zero power, with all signals consequentially initialised to zero.

### C. Discrete Current Controller Model

The discrete time synchronous reference frame current controller is modelled by the basic macros of the DIgSILENT Power Factory library, as shown in Fig. 8. The DIgSILENT Power Factory does not provide an option for an in built discrete time integrator similar to the PSIM model of Fig. 3. Instead, this is implemented in this study by the forward Euler discrete integration as given in (6):

$$y(n) = y(n-1) + T * u(n-1) \quad (6)$$

The discrete-time integration of Fig. 3 with the Forward Euler implementation of (6) is shown in Fig. 8. The variables are initialized from right to left, because the outputs are known, and the inputs have to be determined. Note that the initialization of the controller must be done with caution, because of the anti-windup compensation structure. For example, the initialisation routine for the d-axis is as follows:

```
inc(i_err_d) = id_ref-id
inc(md_sat) = i_err_d*Kp
inc(sd5) = sd4
inc(sd4) = sd2*T_s
inc(sd2) = md_sat*T_i
```

## IV. MODEL VALIDATION VIA THE VERIFIED PSIM MODEL

The transient performance of the three-phase grid connected inverter EMT DIgSILENT Power Factory model has been investigated by comparing the inverter side current controller performance of the developed EMT model against that of the known discrete-time PSIM model, simulated with the parameters given in Table I and Table II.

The step-up transient performance was investigated by commanding a step change in the reference signal ( $i_{dref}$ ) from 5A to 10A at  $t=0.025$ s. The results for the inverter side inductor current, the reference tracking current and modulating signals are shown in Fig. 9a, Fig. 10a, Fig. 11a and Fig. 12a. An equivalent reference step change from 0.25 p.u. to 0.50 p.u. was commanded for the DIgSILENT Power Factory EMT model, with its comparative response shown in Fig. 9b, Fig. 10b, Fig. 11b and Fig. 12b.

The step-down transient performance was investigated by commanding a step change in reference signal ( $i_{dref}$ ) from 10A to 7A at  $t=0.17$ s. The PSIM results for the inverter side

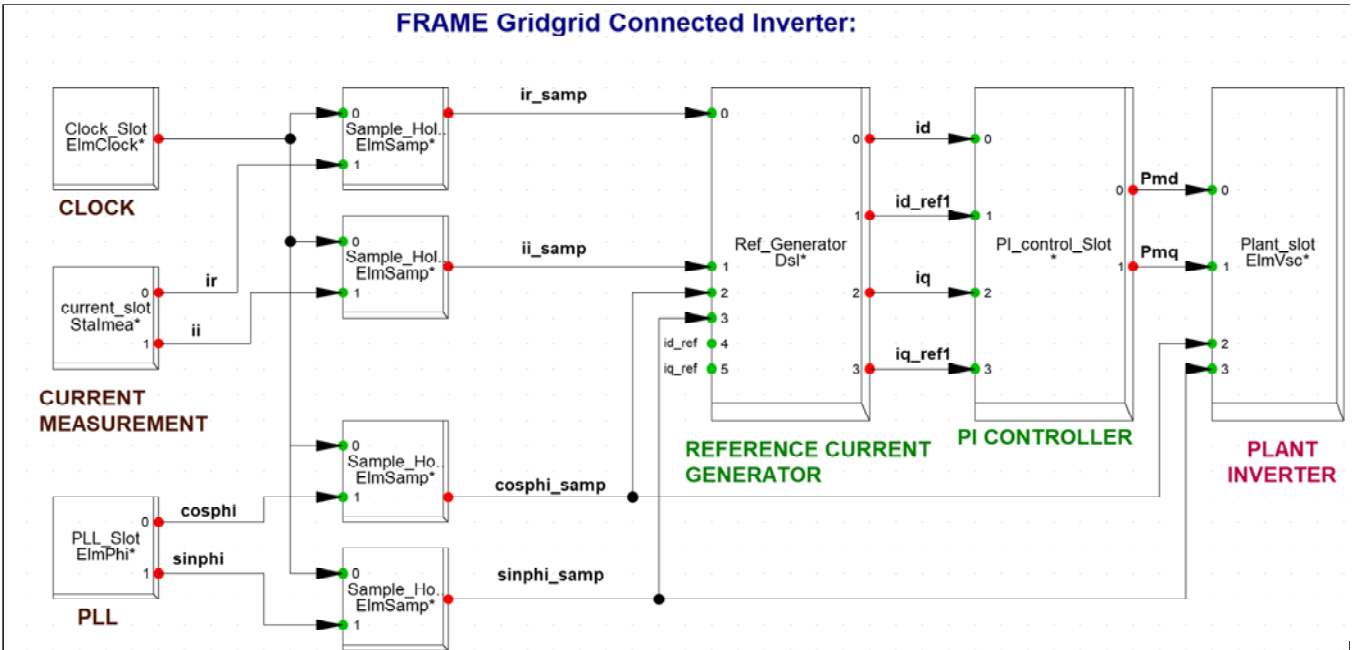


Fig. 6: DiGSILENT Composite Frame of the grid connected inverter with SRF current regulator.

inductor current, the reference tracking current and modulating signals are shown in Fig. 13a, Fig. 14a, Fig. 15a and Fig. 16a. An equivalent reference step change from 0.50 p.u. to 0.35 p.u. was commanded for the DiGSILENT Power Factory EMT model, with its comparative response shown in Fig. 13b, Fig. 14b, Fig. 15b and Fig. 16b.

The results for the two controllers are almost identical, which validates the accuracy of the DiGSILENT model (since the PSIM model is known from previous work to almost exactly match its reference experimental systems)

V. CONCLUSIONS

This paper has presented the development of an accurate DiGSILENT EMT three-phase inverter simulation model. The inverter controllers have been developed in the discrete time-domain and the model has been validated against a detailed time-domain PSIM model (which has been previously referenced to an experimental system). The results show that the DiGSILENT PowerFactory EMT tool can be used to accurately model the transient response of a grid-connected inverter system, if the discrete-time controller of the inverter is correctly constructed using the EMT discrete-time tools.

VI. ACKNOWLEDGEMENT

This paper acknowledges the support of Australian Research Council Discovery Grant DP180103200. The authors would also like to thank Dr Ahmad Afif Nazib, researcher at RMIT, for providing the PSIM base models.

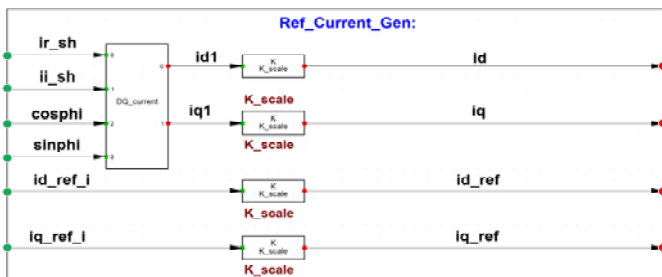


Fig. 7: DiGSILENT common model of reference current generation.

REFERENCES

- [1] H. T. Mokui, M. A. Masoum, and M. Mohseni, "Review on Australian grid codes for wind power integration in comparison with international standards," *2014 Australasian universities power engineering conference (AUPEC)*, 2014: IEEE, pp. 1-6.
- [2] A. Q. Al-Shetwi, M. Hannan, K. P. Jern, M. Mansur, and T. Mahlia, "Grid-connected renewable energy sources: Review of the recent integration requirements and control methods," *Journal of Cleaner Production*, vol. 253, p. 119831, 2020.
- [3] L. M. Castro, J. R. Rodríguez-Rodríguez, and C. Martín-del-Campo, "Modelling of PV systems as distributed energy resources for steady-state power flow studies," *International Journal of Electrical Power & Energy Systems*, vol. 115, p. 105505, 2020/02/01/ 2020, doi: <https://doi.org/10.1016/j.ijepes.2019.105505>.
- [4] G. Lammert *et al.*, "International industry practice on modelling and dynamic performance of inverter based generation in power system studies," *CIGRE Science & Engineering*, vol. 8, pp. 25-37, 2017. J.
- [5] AEMO, "Connection of Large-Scale Solar Farms To Weak Networks," 2017. [Online]. Available: [https://solarintegrationworkshop.org/wp-content/uploads/2019/08/Use-of-Real-Code-in-EMT-Models-IEEE\\_Atlanta.pdf](https://solarintegrationworkshop.org/wp-content/uploads/2019/08/Use-of-Real-Code-in-EMT-Models-IEEE_Atlanta.pdf) (accessed 2020).
- [7] Bowes, C. Booth, and S. Strachan, "System interconnection as a path to bottom up electrification," in *2017 52nd International Universities Power Engineering Conference (UPEC)*, 2017: IEEE, pp. 1-5.
- [8] K. Hackel, C. Farkas, and A. Dán, "Inverter control modeling in DiGSILENT Power Factory Power Factory to analyze the effects of DG units

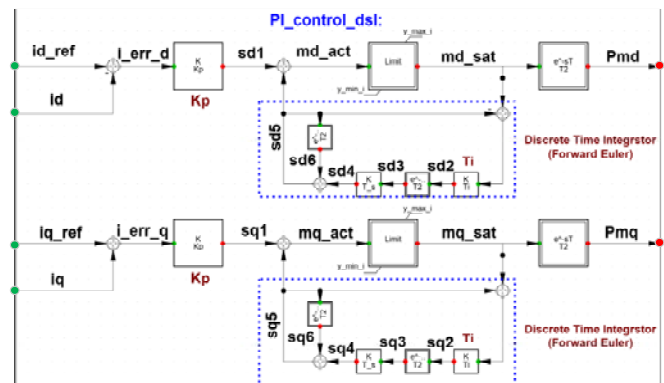


Fig. 8: DiGSILENT common model of PI SRF current regulator DSL.

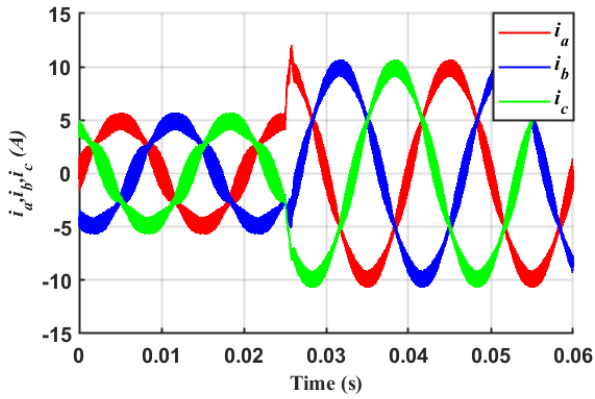


Fig. 9a: Inverter side inductor three phase currents for step increase in input reference (PSIM results)

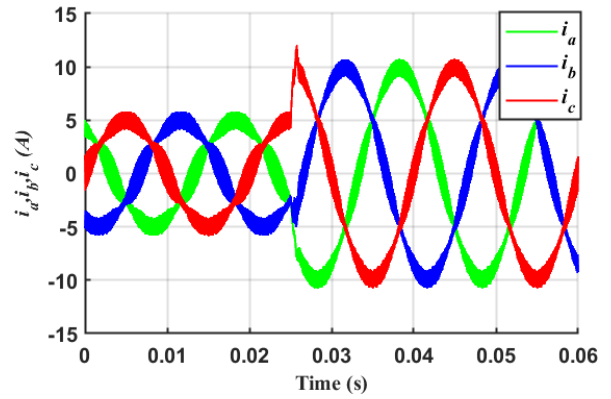


Fig. 9b: Inverter side inductor three phase currents for step increase in input reference (DIgSILENT results)

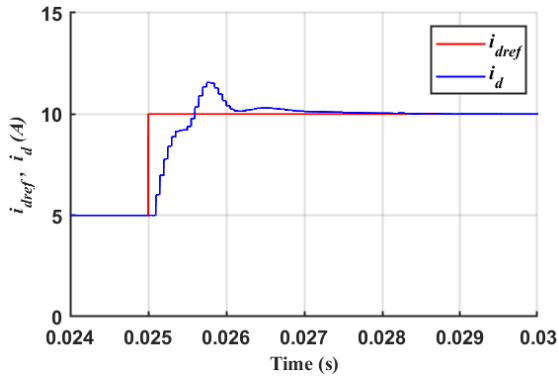


Fig. 10a: Transient performance: for step increase in input reference current (PSIM results)

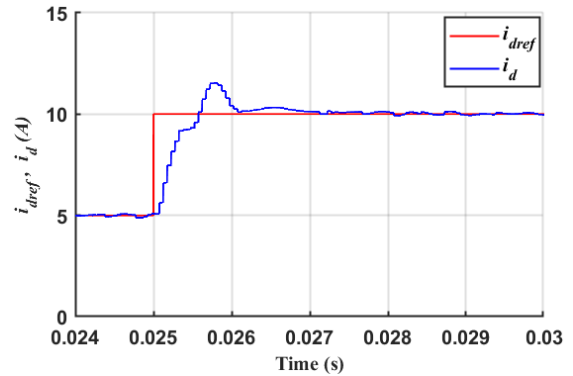


Fig. 10b: Transient performance: for step increase in input reference current (DIgSILENT results)

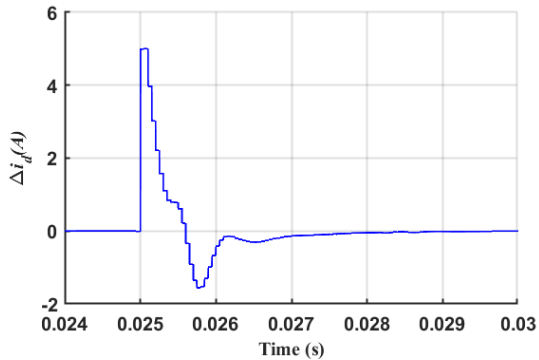


Fig. 11a: Steady state error: for step increase in input reference current (PSIM results)

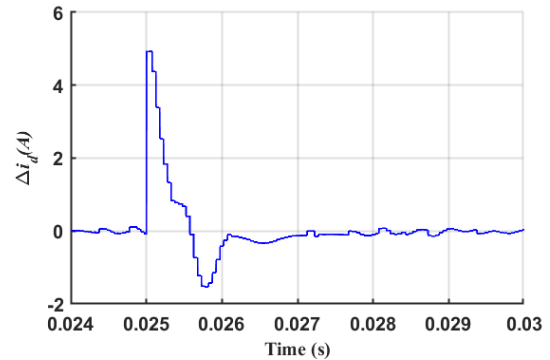


Fig. 11b: Steady state error: for step increase in input reference current (DIgSILENT results)

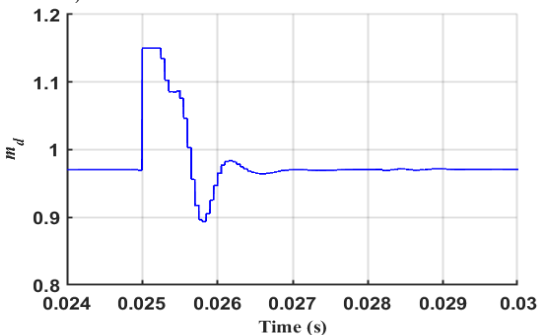


Fig. 12a: Modulating signal: (PSIM results)

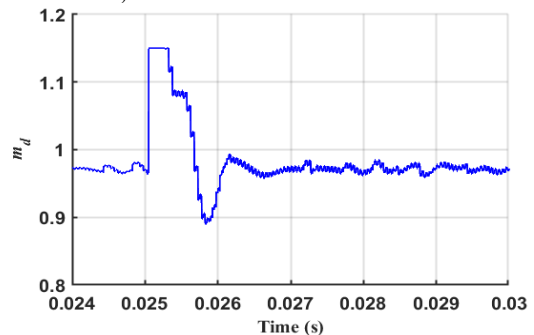


Fig. 12b: Modulating signal: (DIgSILENT results)

on the distribution grid," in *2015 5th International Youth Conference on Energy (IYCE)*, 27-30 May 2015 2015, pp. 1-7, doi: 10.1109/IYCE.2015.7180760.

[9] C. A. Teixeira, D. G. Holmes, B. P. McGrath, P. Sykes, and A. McIver, "A hardware/software co-simulation framework for power converter firmware development," in *2014 IEEE 5th International Symposium on Power Electronics for Distributed Generation Systems*

(PEDG), 24-27 June 2014 2014, pp. 1-8, doi: 10.1109/PEDG.2014.6878704.

[10] R. N. Beres, X. Wang, M. Liserre, F. Blaabjerg, and C. L. Bak, "A review of p passive power filters for three-phase grid-connected voltage-source converters," *IEEE Journal of Emerging and Selected Topics in Power Electronics*, vol. 4, no. 1, pp. 54-69, 2015.

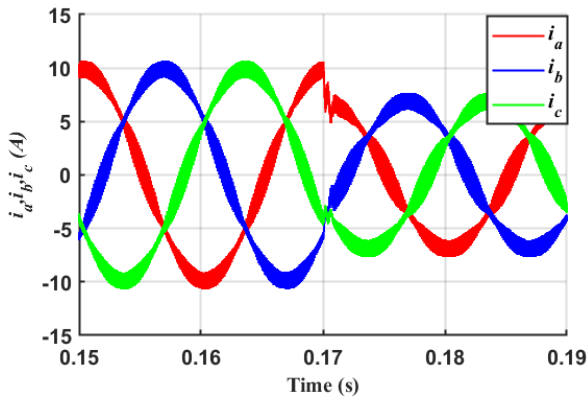


Fig. 13a: Inverter side inductor three phase currents for step decrease in input reference (PSIM results)

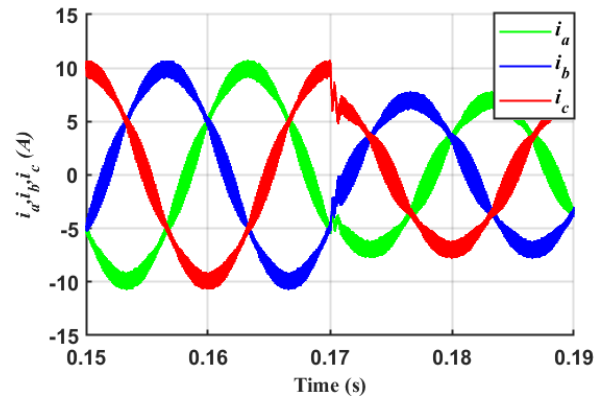


Fig. 13b: Inverter side inductor three phase currents for step decrease in input reference (DIgSILENT results)

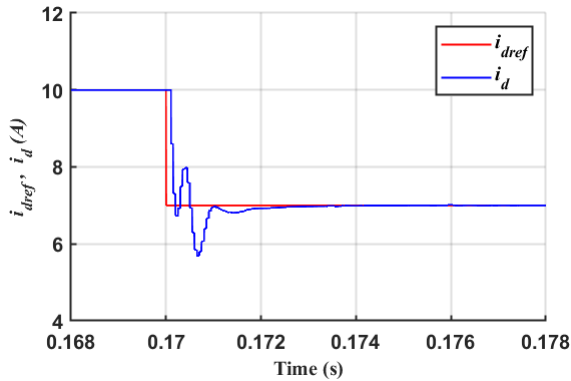


Fig. 14a: Transient performance: for step decrease in input reference current (PSIM results)

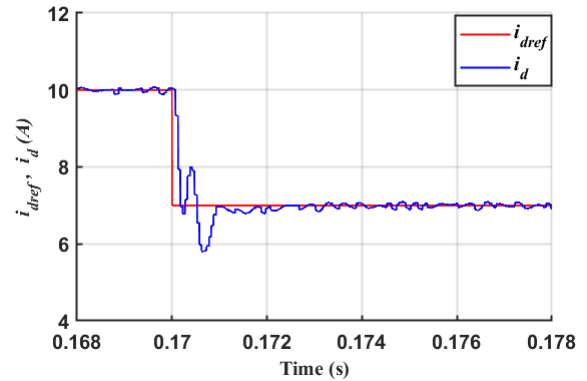


Fig. 14b: Transient performance: for step decrease in input reference current (DIgSILENT results)

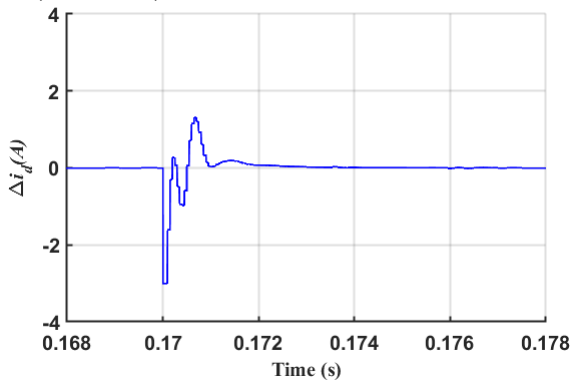


Fig. 15a: Steady state error: for step decrease in input reference current (PSIM results)

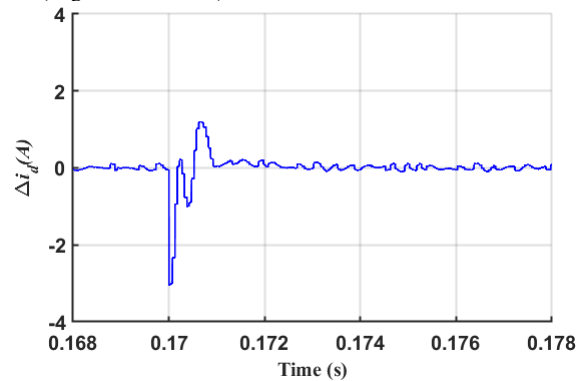


Fig. 15b: Steady state error: for step decrease in input reference current (DIgSILENT results)

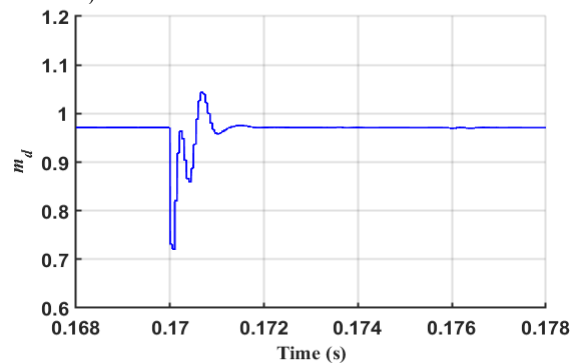


Fig. 16a: Modulating signal: for step decrease in input reference current (PSIM results)

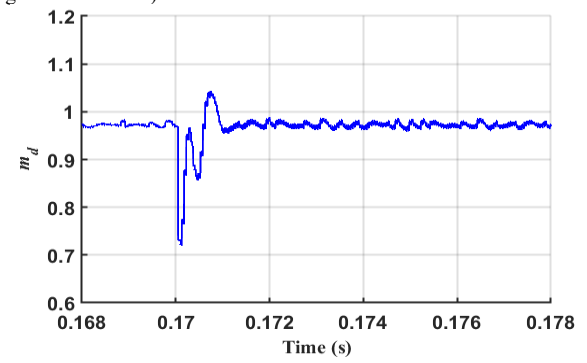


Fig. 16b: Modulating signal: for step decrease in input reference current (DIgSILENT results)

[11] D. G. Holmes, T. A. Lipo, B. P. McGrath, and W. Y. Kong, "Optimized Design of Stationary Frame Three Phase AC Current Regulators," *IEEE Transactions on Power Electronics*, vol. 24, no. 11, pp. 2417-2426, 2009, doi: 10.1109/TPEL.2009.2029548.

[12] B. P. McGrath and D. G. Holmes, "Anti-windup control for stationary frame current regulators using digital conditioning architectures," in *2017 IEEE Energy Conversion Congress and Exposition (ECCE)*, 1-5 Oct. 2017 2017, pp. 5744-5751, doi: 10.1109/ECCE.2017.8096954J.